Journal of Integrative Agriculture 2026, 25(2): 424–435

Available online at ScienceDirect

Journal of Integrative Agriculture



RESEARCH ARTICLE

Variations and major driving factors for soil nutrients in a typical karst region in Southwest China

Miaomiao Wang[1, 2], Hongsong Chen[2, 3#], Wei Zhang[2, 3], Kelin Wang[2, 3]

[1] *College of Life and Environmental Science, Central South University of Forestry and Technology, Changsha 410004, China*
[2] *Institute of Subtropical Agriculture, Chinese Academy of Sciences, Changsha 410125, China*
[3] *Guangxi Key Laboratory of Karst Ecological Processes and Services, Huanjiang Observation and Research Station for Karst Ecosystems, Chinese Academy of Sciences, Huanjiang 547100, China*

Highlights

- SOC, TN, TP, and TK concentrations exhibited moderate variations in soil and obvious positive spatial autocorrelations.
- Terrestrial ecosystems in the study area were more vulnerable to soil P and K than soil N deficiencies.
- Other soil properties accounted more for variations in soil nutrient concentrations than spatial and environmental variables.

Abstract

Understanding the spatial distributions and corresponding variation mechanisms of key soil nutrients in fragile karst ecosystems can assist in promoting sustainable development. However, due to the implementation of ecological restoration initiatives such as land-use conversions, novel changes in the spatial characteristics of soil nutrients remain unknown. To address this gap, we explored nutrient variations and the drivers of the variation in the 0–15 cm topsoil layer using a regional-scale sampling method in a typical karst area in northwest Guangxi Zhuang Autonomous Region, Southwest China. Descriptive statistics, geostatistics, and spatial analysis were used to assess the soil nutrient variability. The results indicated that soil organic carbon (SOC), total nitrogen (TN), total phosphorus (TP), and total potassium (TK) concentrations showed moderate variations, with coefficients of variance being 0.60, 0.60, 0.71, and 0.72, respectively. Moreover, they demonstrated positive spatial autocorrelations, with global Moran's indices being 0.68, 0.77, 0.64, and 0.68, respectively. However, local Moran's index values were low, indicating large spatial variations in soil nutrients. The best-fitting semi-variogram models for SOC, TN, TP, and TK concentrations were spherical, Gaussian, exponential, and exponential, respectively. According to the classification criteria of the Second National Soil Census in China, SOC and TN concentrations were relatively sufficient, with the proportions of rich and very rich levels being up to 90.9 and 96.0%, respectively. TP concentration was in the medium-deficient level, with the areas of medium and deficient levels accounting for 33.7 and 30.1% of the total, respectively. TK concentration was deficient, with the cumulative area of extremely deficient, very deficient, and deficient levels accounting for 87.6% of the total area. Consequently, the terrestrial ecosystems in the study area were more vulnerable to soil P and K than soil N deficiencies. Furthermore, variance partitioning analysis of the influencing factors showed that, except for the interactions, the single effect of other soil properties accounted more for soil nutrient variations than spatial and environmental variables. These results will aid in the future management of terrestrial ecosystems.

Keywords: dominant factor, geostatistics, karst ecosystem, soil nutrient classification, spatial variation

1. Introduction

Soil is the basis for global and regional processes and functions such as land degradation, water cycling, biodiversity conservation, carbon sequestration, and maintaining ecosystem quality (Liu *et al.* 2022). Soil carbon (C), nitrogen (N), phosphorus (P), and potassium (K) are

Received 9 December 2024; Received in revised form 10 February 2025; Accepted 9 March 2025; Available online 4 April 2025
Miaomiao Wang, E-mail: miaomiaowang@csuft.edu.cn; #Correspondence Hongsong Chen, E-mail: hbchs@isa.ac.cn

© 2026 CAAS. Publishing services by Elsevier B.V. on behalf of KeAi Communications Co. Ltd. This is an open access article under the CC BY-NC-ND license (http://creativecommons.org/licenses/by-nc-nd/4.0/). Peer review under responsibility of Editorial Board of *Journal of Integrative Agriculture*.
doi: 10.1016/j.jia.2025.04.010

competitive macro-elements for plants and microorganisms and critical indices of soil fertility (Li *et al.* 2020). Generally, soil nutrient distribution is influenced by various factors such as topography (Wang M R *et al.* 2021), regional and global climate (Tan *et al.* 2020; Zhu *et al.* 2021), soil physicochemical properties (Wang *et al.* 2019), soil microorganisms (Chen *et al.* 2018), geographic location (Maila *et al.* 2006; Wen and He 2016), and human activities (Huang *et al.* 2020). In addition, the effects of influencing factors on different soil nutrient elements vary owing to differences in the magnitudes and directions of the effects. The impacts and interactions of numerous influencing factors on soil nutrients are extremely complex and exhibit high regional variation. Consequently, a comprehensive understanding of the spatial distribution characteristics of soil nutrients and their driving factors in a specific area is necessary to facilitate sustainable ecosystem management.

The interrelationships and characteristics of different soil nutrients play important roles in various ecological processes (Wang *et al.* 2023). Previous studies have indicated that the rate of soil organic carbon (SOC) accumulation significantly depends on the net primary productivity of plants, which in most ecosystems is primarily limited by N (Jobbágy and Jackson 2000). As major components of the global C and N cycles, SOC and soil total N (TN) interact and influence the proportion of atmospheric greenhouse gases and consequently global climate change (Wang X Y *et al.* 2021). P is a vital element in the biological systems of the Earth and a major limiting nutrient for plant growth and ecosystem development (Zhu *et al.* 2021). The occurrence of P in soil is predominantly due to lithospheric minerals, which are released by weathering and chemically transformed within the pedosphere into a dissolved state that finally enters the food chain *via* plant roots (Filippelli 2008). N enrichment temporarily buffers ecosystem P limitation, but can extensively deplete soil P pools in the long term (Wang X Y *et al.* 2021). Along with soil C, N, and P, K is important for terrestrial ecosystems, but in comparison, it has not been as widely studied. The exogenous source of K in most terrestrial ecosystems is rock weathering, whereas the source of K in soil is cation exchange sites (Schlesinger 2021). Although TN, TP, and TK cannot be directly used by plants, considering their relative stability and correlation with available nutrients, understanding the spatial patterns of SOC, TN, TP, and TK, and quantifying the contributions of different influencing factors can provide a scientific reference for sustainable soil utilization and rational intervention.

Generally, SOC and TN concentrations show similar spatial patterns with complex regional variations. For example, Tang *et al.* (2018) estimated C pools in China by conducting an intensive field survey and found the highest soil C density on Mount Xing'an in the northeastern region, Mounts Qilian and Bayan Har in Qinghai, and Mounts Tianshan and Alta in northern Xinjiang, followed by the southern and southeastern regions, whereas the lowest soil C density was observed in the lower basins of Xinjiang, Hexi Corridor in Gansu, and parts of the Loess Plateau. In addition, the C densities of forests, shrublands, and grasslands decreased with increasing temperature but increased with increasing precipitation. Zhou *et al.* (2020) compiled a 90-m resolution map of soil TN in China using weighted model averaging and showed that high-value areas of soil TN were predominantly distributed in the eastern Tibetan Plateau, central Qilian Mountains, and north Greater Khingan Range. Moreover, climatic factors considerably influenced the variation in soil TN. However, unlike the soil C and N coupling, changes of P and K in soil varied. For example, Zhu *et al.* (2021) conducted an intensive field investigation in different forest ecosystems in China to assess TP, and concluded that it increased with increasing latitude and elevation but decreased with increasing longitude; furthermore, the combined effect of temperature and precipitation was the most important factor. Duan *et al.* (2020) determined the spatial variability of TK in paddy fields in Hunan Province, and showed that TK concentration was relatively high in the southern areas. In summary, soil nutrient distributions are sensitive to changes in regional climate and topography. Comparatively, at the small watershed scale, soil physicochemical properties and microbial composition are the main drivers of soil nutrient variations (Osburn *et al.* 2021; Yang *et al.* 2021).

Most ecosystems currently have low productivity because of soil nutrient loss, which consequently decreases their ability to maintain sustainability (Meng *et al.* 2021). This problem occurs most prominently in fragile ecosystems. Karst ecosystems are typically fragile habitats that are highly susceptible to serious damages and cannot be easily restored (Tang *et al.* 2019). The soil in such ecosystems is shallow and discontinuous (Jiang *et al.* 2014), and the high levels of heterogeneity increase the importance of the spatial characteristics of soil properties, especially soil nutrients. Moreover, soil nutrients in such areas can change because of land use conversions (Wang *et al.* 2018), which result in variations in the spatial distribution characteristics of nutrients at a regional scale. The karst region in Southwest China is one of the largest continuous karst regions worldwide (Zhang *et al.* 2017). Recently, because of the increasing importance attached to its living environment, ecological restoration efforts such as China's Grain to Green Program (GTGP), have been implemented to improve ecosystem services in karst regions (Zhang *et al.* 2015). As the current fragile ecosystems are unsustainable, clarifying the novel variation characteristics of soil nutrients and the corresponding dominant drivers of the variations is necessary to improve management practices and ecosystem service functions (Haruna 2021).

Geostatistical and spatial analyses involving spatial modeling (variography), spatial interpolation (kriging), and Moran's index calculation have been extensively used to reveal the spatial variabilities in soil physical, chemical, and biological properties (Jiang *et al.* 2020; Wang *et al.* 2020; Haruna 2021; Wang M R *et al.* 2021; Wang X Y *et al.* 2021; Xie *et al.* 2021). Researches on peak-cluster depression karst ecosystems have majorly focused on small watershed or transect scales (Liu *et al.* 2015; Chen *et al.* 2018; Hu *et al.* 2022), with few studies on the spatial variability of soil nutrients at large planar scales. To address this gap, we explored soil nutrient variations and driving factors at the regional scale in a typical karst region in the northwest

Guangxi Zhuang Autonomous Region, Southwest China. Specifically, to clarify the soil nutrient status after the implementation of a series of ecological restoration projects, the aims of this study were to: 1) visualize the spatial distribution characteristics and levels of soil nutrients; and 2) identify the dominant factors causing soil nutrient variations and quantify their relative contributions. An understanding of the spatial variation characteristics of soil nutrients and dominant drivers of variations can help improve the management of soil ecosystem services.

2. Materials and methods

2.1. Study area

The study area (23°35′–25°33′N, 107°20′–109°10′E), which included Huanjiang, Luocheng, Du'an, and Dahua counties, and Hechi and Yizhou districts, is located in the northwest Guangxi Zhuang Autonomous Region, Southwest China (Fig. 1). The region is characterized by a subtropical monsoon climate with a mean air temperature (MAT) of 17.8–22.2ºC and mean annual precipitation (MAP) of 1,346–1,640 mm. The topography is complex and variable, with a typical peak-cluster depression landform. The soils are Calcisols over dolomite or limestone in karst areas and Ferralsols over clasolite in non-karst areas (WRB 2015). Based on the universality and impact of ecological restoration projects such as GTGP, five land use types were sampled: secondary forest, plantation forest, shrubland, grassland, and cropland. The secondary forest was dominated by macrophanerophytes such as *Sinoadina racemosa* and *Radermachera sinica*; plantation forest included *Zenia insignis* Chun and other economically important species; shrubland was predominantly inhabited by *Vitex negundo* L. and *Pterolobium punctatum* Hemsl; grassland was dominated by Gramineae such as *Imperata cylindrica* and *Miscanthus floridulus*; and cropland was typically managed under a corn–soybean rotation.

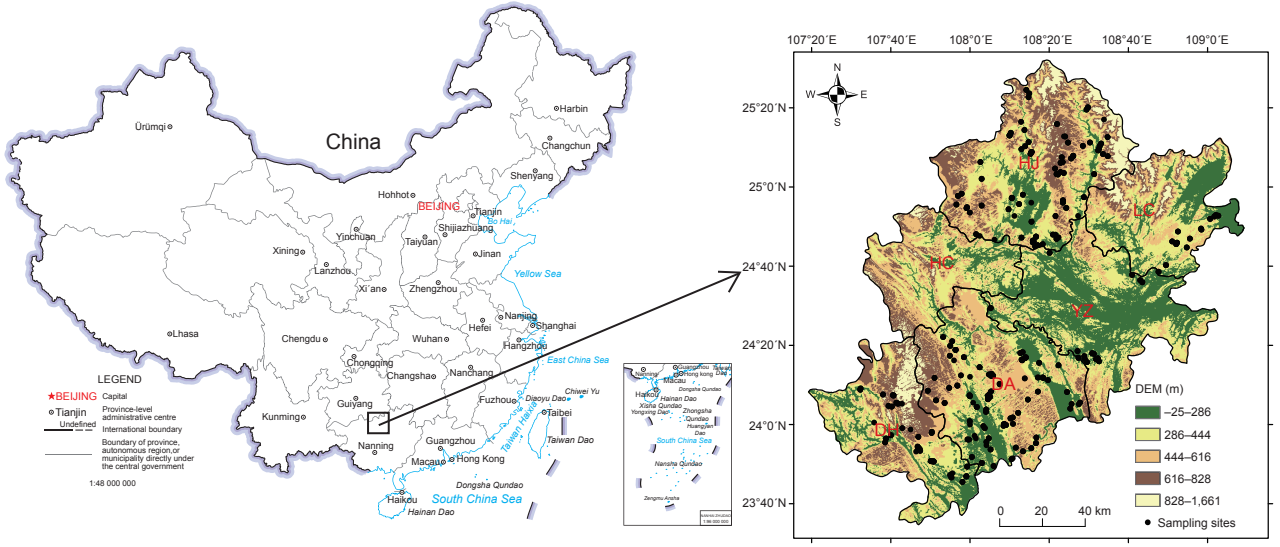
2.2. Soil sampling and analysis

Considering the typical topography in the study area, four slopes were considered: upper, middle, lower slopes and depression, which were on the same aspect for each study site. The interval between adjacent slopes was at least 30 m. Soil was sampled from the end of March to early June in 2015 and 2016 using a stratified random sampling approach, with lithology, land-use type, and slope position being the primary stratifying factors for site selection. At each site, at least nine soil samples were collected at depths of 0–15 cm from a 20 m×20 m quadrat, and composited to form a single sample. In total, 707 composite soil samples were collected (Table 1). After removing fine roots, soil samples were air-dried and sieved using a 2-mm mesh for further physicochemical analysis including total soil nutrients, pH, soil texture, and exchangeable cation concentrations.

SOC was measured by wet oxidation using the dichromate redox colorimetric method, with which carbonates are not determined (Carter and Gregorich 2006). TN was determined using the Kjeldahl method with a continuous flow analyzer (AutoAnalyzer-AA3; Seal Analytical, Norderstedt, Germany) (Gallaher *et al.* 1976). Finally, TP and TK were measured using an ultraviolet spectrophotometer (Lambda 25, Perkin Elmer, Singapore) and atomic absorption spectrometer (PE, AAnalyst 800, USA), respectively, after NaOH fusion (Wang *et al.* 2018; Duan *et al.* 2020).

2.3. Determination of influencing factors

Bulk density (BD) and soil moisture content (SMC) were determined using the cutting ring method (Zhang *et al.* 2014), whereas bare rock rate (BRR) was estimated during sampling using the ratio of the area covered by rock to the total survey area. Soil texture (clay, silt, and sand contents) was determined using a laser diffraction particle size analyzer (Mastersizer 2000, Malvern, UK) and classified according to USDA classification (Liu *et al.* 2015). Soil pH (1:2.5 soil/



审图号：GS 京 (2025) 2380 号

Fig. 1 Location of the study area and sampling sites. DEM, digital elevation model; HJ, Huanjiang County; LC, Luocheng County; HC, Hechi District; YZ, Yizhou District; DA, Du'an County; DH, Dahua County.

Table 1 Number of sampling sites for each lithology, land-use type, and slope position

	Land-use type					Total
	Secondary forest	Shrubland	Grassland	Cropland	Plantation forest	
Lithology						
Dolomite	52	53	56	59	40	260
Limestone	59	65	63	73	68	328
Clasolite	6	–	3	53	57	119
Total	117	118	122	185	165	707
Slope position						
Up slope	37	37	40	55	51	220
Middle slope	40	39	39	57	56	231
Down slope	39	40	41	61	56	237
Depression	1	2	2	12	2	19
Total	117	118	122	185	165	707

water ratio) was measured using a pH meter (FE20K, Mettler-Toledo, Switzerland). The exchangeable calcium (Ca^{2+}) and magnesium (Mg^{2+}) were displaced *via* compulsive exchange in 1 mol L^{-1} ammonium acetate at pH 7.0 and analyzed by atomic absorption spectrometry (NOVAA 350).

Data on lithology, land-use type, slope position, and soil depth (SD) were recorded during sampling. Topographic metrics (elevation, slope, and aspect) were obtained from a digital elevation model with a spatial resolution of 30 m×30 m using ArcGIS 10.3 (ESRI, Inc., USA). The normalized difference vegetation index (NDVI) was generated from a Thematic Mapper image at a spatial resolution of 30 m×30 m, with minimal cloud cover during the growing season. The topographic wetness index (TWI), proposed by Beven and Kirkby (1979), was calculated using the formula: TWI=ln(α/tanβ), where α is the specific upslope area and tanβ is the local slope. NDVI and TWI were calculated using ArcGIS software. MAT and MAP data were obtained from the Data Center for Resources and Environmental Sciences, Chinese Academy of Sciences (http://www.resdc.cn).

Spatial variables included the latitudinal (x) and longitudinal (y) coordinates of each sampling location, and their higher and cross-produced terms (xy, x^2, y^2, x^2y, xy^2, x^3, and y^3) generated from the cubic trend surface analysis (Heikkinen *et al.* 2004; Chen *et al.* 2017). These spatial variables were used to present the spatial structure and were also a proxy for the underlying effects of temperature and precipitation in the study region.

2.4. Statistical analysis methods

Descriptive statistical analysis was used to determine the mean, standard deviation, coefficient of variance (CV), skewness, and kurtosis of soil nutrient concentrations (Luo *et al.* 2021). Data were checked for normality and homogeneity of variance and were transformed if necessary. The soil nutrient data used for geostatistical analysis were transformed by natural logarithm to follow a normal distribution. One-way analysis of variance (ANOVA) was used to determine the significance of land use, lithology, and slope position effects on other variables. SPSS 21.0 (SPSS Inc., Chicago, IL, USA) was used for statistical analyses. Geostatistical analysis (semi-variogram analysis) was performed using GS+ (Gamma Design Software). Spatial variables (x, y, xy, x^2, y^2, x^2y, xy^2, x^3, and y^3), other soil properties (SMC, BD, pH, clay, silt, sand, Ca^{2+}, and Mg^{2+}), and environmental factors (lithology, land-use type, slope position, BRR, SD, elevation, slope, aspect, NDVI, TWI, MAT, and MAP) were considered while selecting the significant influencing factors on soil nutrients. Redundancy analysis (RDA) and variance partitioning analysis (VPA) of these factors were performed using Canoco 5.0 (http://www.canoco5.com/). In the data set of explanatory variables for VPA, three groups: spatial variables, other soil properties, and environmental factors were divided to calculate their single and interactive effects on soil nutrient variations. Soil nutrient levels were determined according to the classification criteria of the Second National Soil Census in China (Table 2), which occurred from 1979 to 1986 and generated a series of results of soil data for China.

Spatial analysis (the global and local Moran's indices) was used to describe the spatial characteristics of soil nutrients (Wang *et al.* 2020). The global Moran's index (GMI), a spatial autocorrelation coefficient, was used to determine spatial autocorrelation. The values ranged from −1 to +1. A GMI>0 indicates a positive spatial correlation; the larger the value, the greater the spatial correlation. Conversely, a GMI<0 indicates a negative spatial correlation; the smaller the value, the greater the spatial difference. A GMI=0 indicates a random spatial distribution. The local Moran's index (LMI) is a decomposition

Table 2 Soil nutrient classifications based on the Second National Soil Census in China

Soil nutrient (g kg^{-1})[1)]	Level 1 (very rich)	Level 2 (rich)	Level 3 (medium)	Level 4 (deficient)	Level 5 (very deficient)	Level 6 (extremely deficient)
SOC	>23	17–23	12–17	6–12	3–6	<3
TN	>2	1.5–2	1–1.5	0.75–1	0.5–0.75	<0.5
TP	>1	0.8–1	0.6–0.8	0.4–0.6	0.2–0.4	<0.2
TK	>25	20–25	15–20	10–15	5–10	<5

[1)] SOC, soil organic carbon; TN, total nitrogen; TP, total phosphorous; TK, total potassium.

form of the GMI. High values indicate that area units with similar variable values (high or low values) are clustered spatially, whereas low values indicate that area units with dissimilar variables are clustered spatially. ArcGIS 10.3 (ESRI, Inc., USA) was used for spatial analysis.

3. Results

3.1. Descriptive statistics of soil nutrient

The ranges of SOC, TN, TP, and TK concentrations were 6.39–109.04, 0.56–10.88, 0.06–3.58, and 0.24–34.68 g kg^{-1}, respectively, with average values of 27.9, 3.0, 0.7, and 8.3 g kg^{-1}, respectively (Fig. 2-A–D). SOC and TN were relatively stable and showed a consistent degree of variation, with the CVs of 0.60, whereas degrees of TP and TK variations were larger, with the CVs reaching 0.71 and 0.72, respectively. Nevertheless, SOC, TN, TP, and TK all showed moderate variations (0.1<CV<1).

3.2. Spatial autocorrelation and variability of soil nutrients

Spatial autocorrelation of soil nutrients The GMI values for SOC, TN, TP, and TK were 0.68, 0.77, 0.64, and 0.68, respectively (Fig. 3-A–D), showing obvious positive spatial autocorrelation. The LMI values of SOC, TN, TP, and TK were low; that is, the area units with dissimilar variables assembled spatially and showed large spatial variations.

Semi-variogram model of soil nutrients The best-fitting semi-variogram models for SOC, TN, TP, and TK were spherical, Gaussian, exponential, and exponential, respectively, with fitting degrees (R^2) of 0.575, 0.519, 0.450, and 0.492, respectively (Table 3). The residual sum of squares (RSS) values were all close to 0. The nugget-sills of SOC, TN, and TP were 14.9, 14.0, and 6.8%, respectively, showing a strong spatial autocorrelation ($C_0/(C_0+C)$<25%), whereas that of TK was 32.7%, indicating a medium degree of spatial autocorrelation (25%<$C_0/(C_0+C)$<75%). The ranges for SOC, TN, TP, and TK were 3.6, 1.7, 1.4, and 1.8 km, respectively.

3.3. Spatial distributions of soil nutrients

Spatial distribution characteristics of soil nutrients SOC concentrations were high in the northeast and relatively low

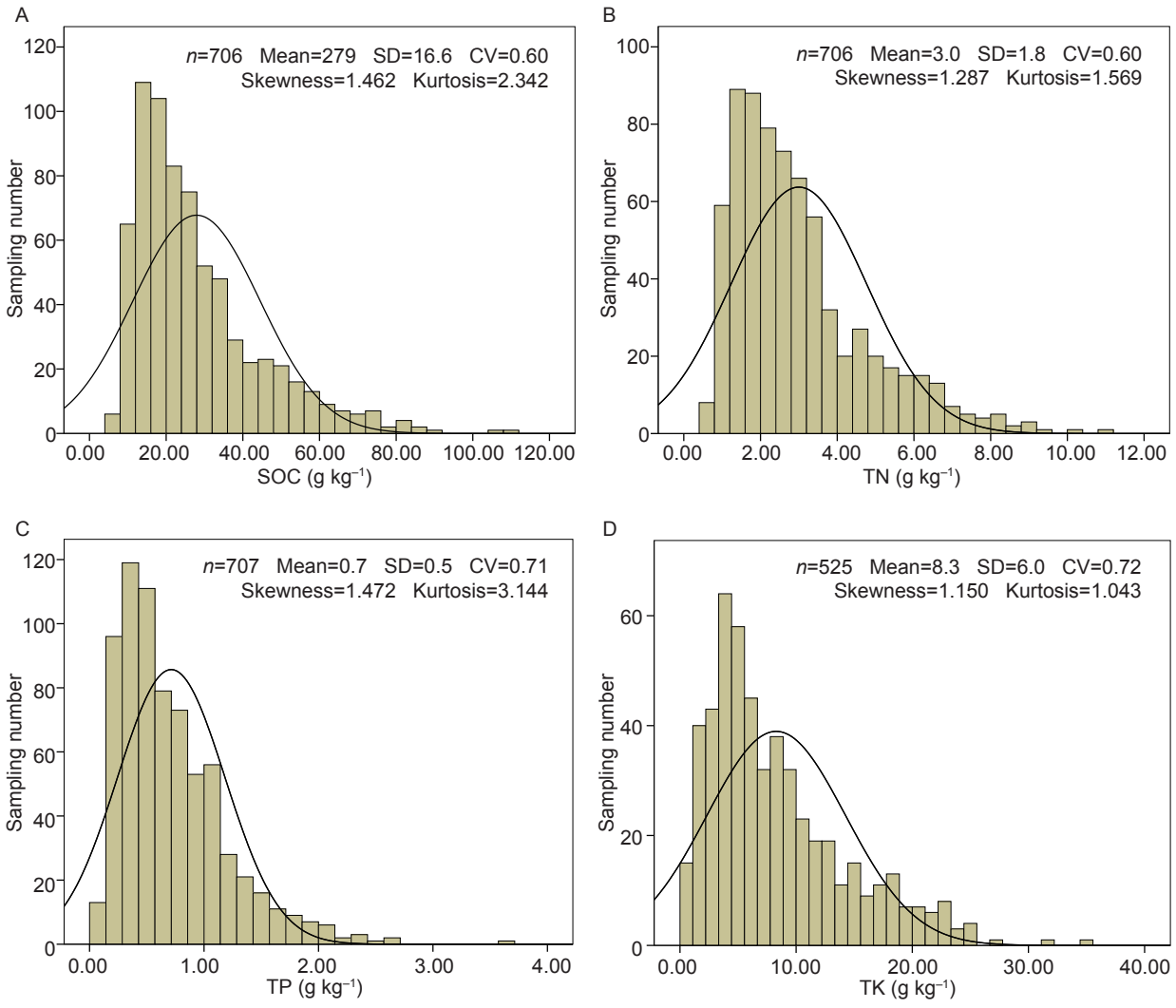
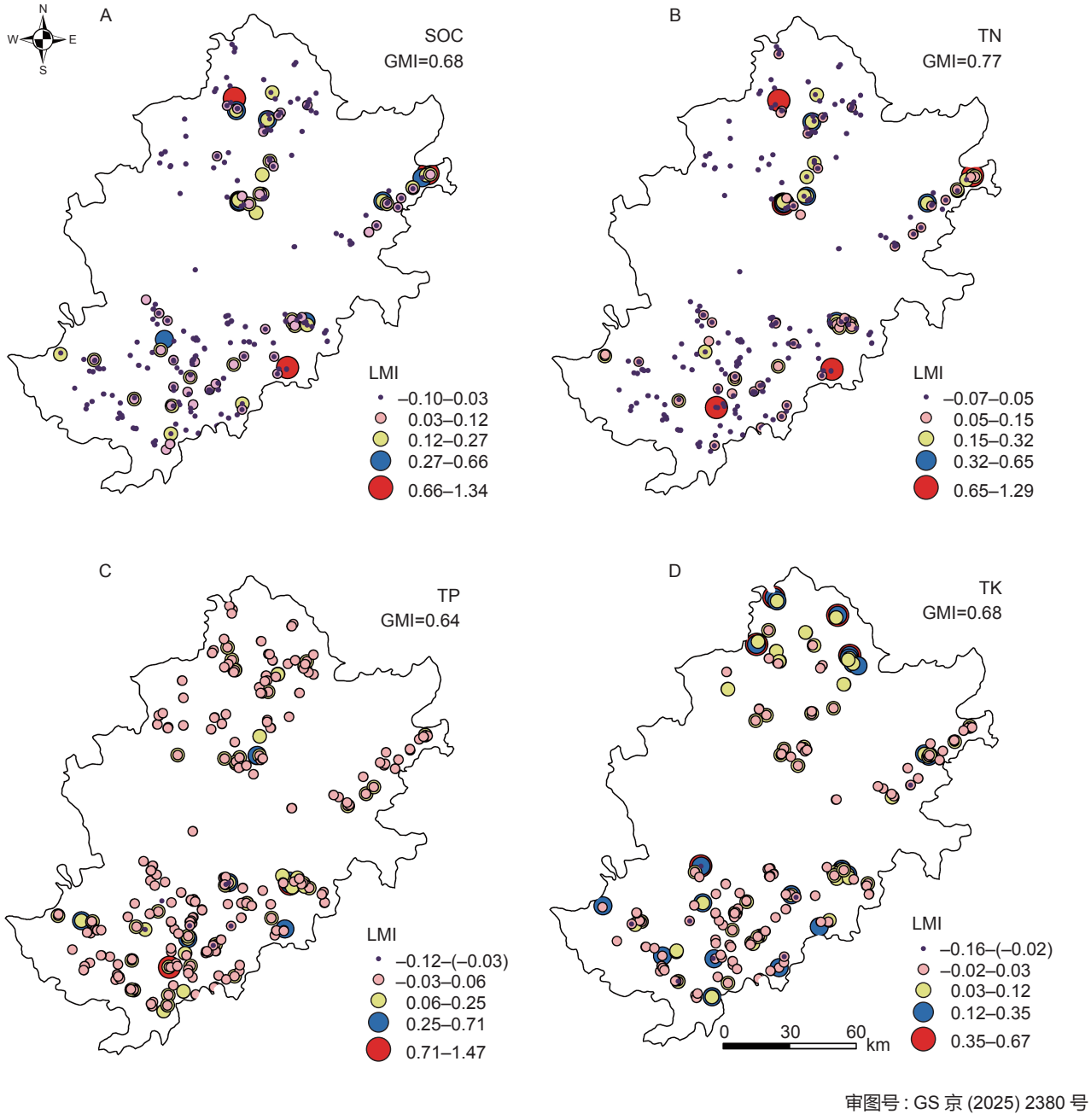


Fig. 2 Descriptive statistics for soil organic carbon (SOC; A), total nitrogen (TN; B), total phosphorous (TP; C), and total potassium (TK; D) concentrations.

at the edges and in the south (Fig. 4-A). A similar distribution was observed for TN, but the patch distribution of TN was more obvious (Fig. 4-B). Furthermore, the range of TP concentrations was relatively stable (most in 0.42–1.10 g kg^{-1}) (Fig. 4-C). Extremely high or low values of TP were rare; specifically, high values were sporadic whereas low values had



审图号 : GS 京 (2025) 2380 号

Fig. 3 Global Moran's index (GMI) and local Moran's index (LMI) of soil organic carbon (SOC; A), total nitrogen (TN; B), total phosphorous (TP; C), and total potassium (TK; D).

Table 3 Semi-variogram models of SOC, TN, TP, and TK and related parameters

Nutrient (Ln)[1)]	Model	Nugget (C_0)	Sill (C_0+C)	Nugget-sill (C_0/(C_0+C))	Range (m)	R^2	RSS[2)]
SOC	Spherical	0.0400	0.2692	0.149	3,600	0.575	3.887E-04
TN	Gaussian	0.0400	0.2850	0.140	1,700	0.519	3.027E-04
TP	Exponential	0.0260	0.3850	0.068	1,400	0.450	2.946E-03
TK	Exponential	0.1820	0.5560	0.327	1,800	0.492	0.0291

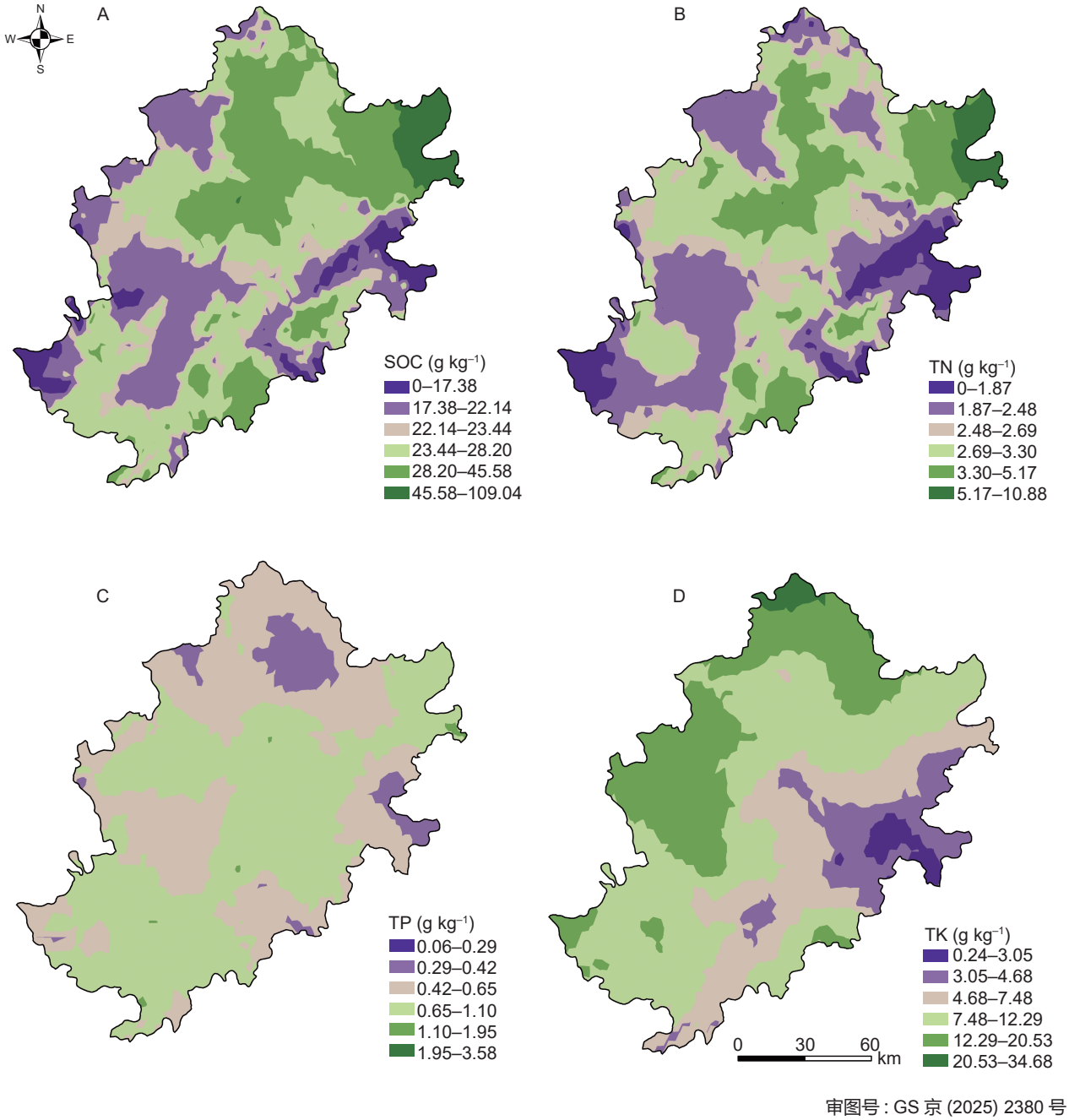
[1)] SOC, soil organic carbon; TN, total nitrogen; TP, total phosphorous; TK, total potassium. Soil nutrient data were transformed by natural logarithm (ln) to follow a normal distribution.
[2)] RSS, the residual sum of squares.

a limited distribution in the north. High and low TK values were distributed in the west and east, respectively; moreover, the TK concentrations in the middle regions ranged from 4.68 to 12.29 g kg^{-1} (Fig. 4-D).

Spatial distributions of soil nutrient levels SOC concentrations were largely sufficient, as none of the examined areas were found to have very deficient or extremely deficient levels (Fig. 5-A); moreover, areas with rich and very rich levels accounted for 90.9% of the total (Table 4). TN classification was similar to that of SOC; the area of very rich level accounted for 82.6% of the total, with the areas of rich and very rich levels in combination accounting for 96.0% of the total (Fig. 5-B). TP was present at all levels with obvious patch characteristics; however, the area of extremely deficient level was close to 0. Furthermore, a large proportion of the area had medium (33.7%) and deficient levels (30.1%), whereas the area of very rich level accounted for only 8.5% (Fig. 5-C). TK did not exhibit the very rich level and was generally reported as being lacking. The cumulative area with extremely deficient, very deficient, and deficient levels accounted for 87.6% of the total. In addition, a very lacking–extremely lacking transitional distribution was observed from west to east, and the medium or rich levels were restricted to the northwest edge (Fig. 5-D).

3.4. Factors influencing soil nutrient variations

The RDA results showed that BD, pH, lithology, clay



审图号 : GS 京 (2025) 2380 号

Fig. 4 Spatial distribution characteristics of soil organic carbon (SOC; A), total nitrogen (TN; B), total phosphorous (TP; C), and total potassium (TK; D).

content, SD, Ca^{2+}, MAT, Mg^{2+}, NDVI, slope position, y^3, y^2, x^3, sand contnet, and slope were significant (P<0.05) factors influencing soil nutrient concentrations by stepwise regression. Among them, SOC and TN were obviously affected by BD, pH, SD, Ca^{2+}, Mg^{2+}, and sand contnet. Furthermore, TP correlated with pH, Mg^{2+}, and sand contnet

Table 4 Area and proportion of different soil nutrient levels[1)]

Soil nutrient level	SOC		TN		TP		TK	
	Area (10^4 km^2)	Proportion (%)	Area (10^4 km^2)	Proportion (%)	Area (10^4 km^2)	Proportion (%)	Area (10^4 km^2)	Proportion (%)
Very rich	1.31	59.1	1.83	82.6	0.19	8.5	0	0
Rich	0.71	31.8	0.30	13.4	0.43	19.3	0.06	2.7
Medium	0.18	8.2	0.08	3.5	0.75	33.7	0.21	9.6
Deficient	0.02	0.9	0.01	0.5	0.67	30.1	0.75	33.7
Very deficient	0	0	0	0	0.18	8.3	0.82	36.8
Extremely deficient	0	0	0	0	0	0	0.38	17.1

[1)] SOC, soil organic carbon; TN, total nitrogen; TP, total phosphorous; TK, total potassium.

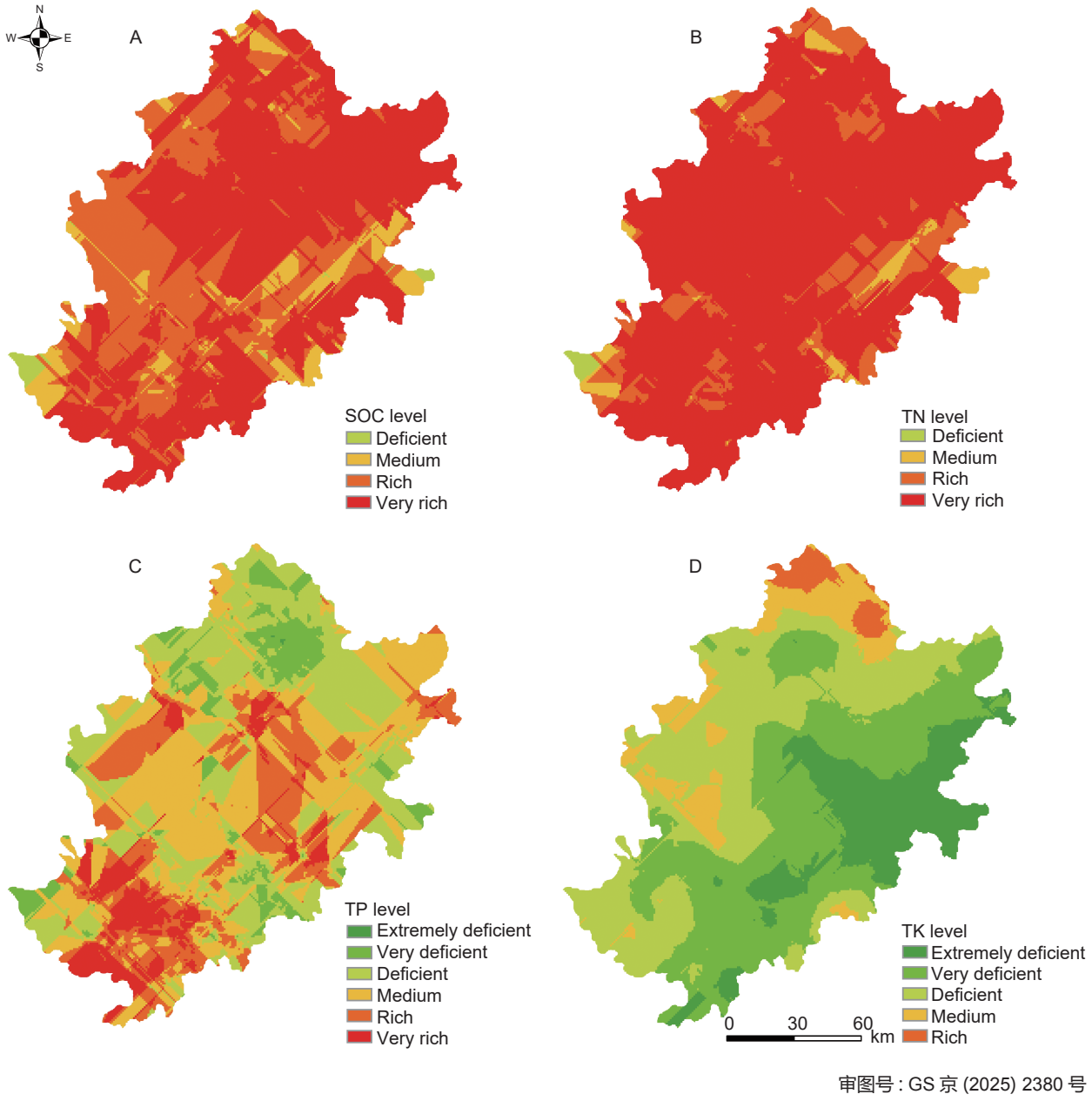


Fig. 5 Spatial distributions of soil organic carbon (SOC; A), total nitrogen (TN; B), total phosphorous (TP; C), and total potassium (TK; D) classifications.

obviously, whereas TK particularly correlated with y^3, y^2, x^3, and MAT (Fig. 6).

According to VPA, considering both single effects and interactions, spatial variables, other soil properties, and environmental factors explained 58.8% of the total variation in soil nutrient concentrations, with the single effect of other soil properties accounting for the largest proportion (29.1%), which was almost half of the total explanation (Fig. 7).

4. Discussion

4.1. Soil nutrients in karst areas

Soil is an important abiotic component of terrestrial ecosystems (Meng *et al.* 2021). Soil nutrient levels, which are key indicators of soil fertility, play a crucial role in regulating plant growth (Huang *et al.* 2020). Karst areas in Southwest China have a unique topography owing to their high landscape heterogeneity and anthropogenic influences (Zhang *et al.* 2017). Moreover, due to shallow and discontinuous soils, the degree of variation in soil nutrients in such areas is greater than that in other regions (Wang *et al.* 2019). In recent years, many ecological restoration projects such as China's GTGP, have been implemented to improve the functions of these fragile ecosystems because of the increased demand for high-quality human living environments, which are generally subject to land-use changes. The results of the present study showed that land use significantly affected levels of SOC, TN, TP, TK, and other variables such as BD, pH, exchangeable cations, and soil texture, which affected soil nutrient levels (P<0.01; Table 5). Thus, it is necessary to elucidate the novel changes in the spatial distribution of soil nutrients resulting from land-use conversions.

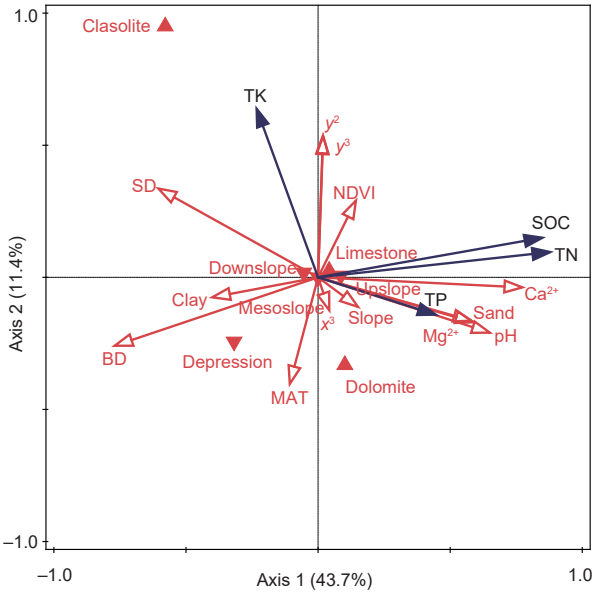


Fig. 6 Redundancy analysis (RDA) of factors influencing soil organic carbon (SOC), total nitrogen (TN), total phosphorous (TP), and total potassium (TK). BD, bulk density; SD, soil depth; NDVI, normalized difference vegetation index; MAT, mean annual temperature; y^2, y^3, and x^3, derived variables of longitude x and latitude y.

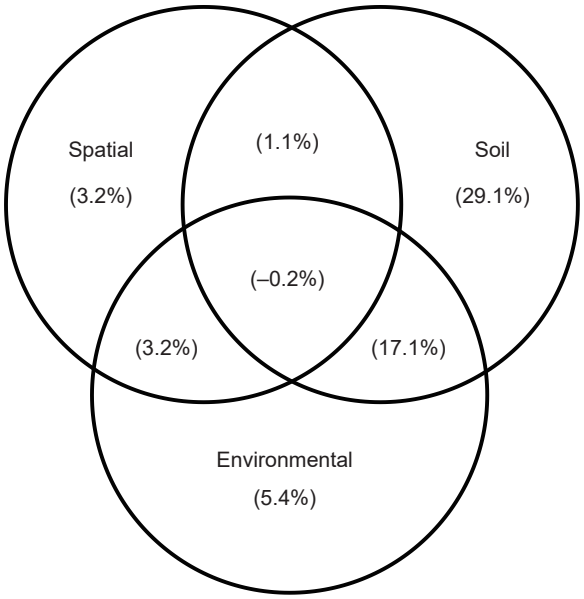


Fig. 7 Variance partitioning analysis (VPA) of spatial variables, other soil properties, and environmental factors for soil nutrient variations. Total explanation=58.8%.

4.2. Characteristics of soil nutrient distributions

Broadly, soil nutrient distributions differ regionally; that is, widespread variations exist (Li *et al.* 2020). These variations are generally due to changes in soil properties, including physicochemical and biological characteristics (Chen *et al.* 2018; Wang *et al.* 2019; Osburn *et al.* 2021; Yang *et al.* 2021) and external environmental factors such as topographic and climatic factors (Li *et al.* 2020; Tan *et al.* 2020; Wang M R *et al.* 2021; Zhu *et al.* 2021). Remarkably, the relative importance of the drivers influencing soil nutrients varies across different regions (Wang R Z *et al.* 2021; Yang *et al.* 2021; Zhu *et al.* 2021); consequently, soil nutrient distributions differ across different regions due to variations in regional characteristics (Duan *et al.* 2020; Wang *et al.* 2020; Haruna *et al.* 2021; Wang R Z *et al.* 2021). Clarifying the adequacy or deficiency of soil nutrients and their dominant influencing factors in each region is fundamental to improving ecosystem sustainability. Overall, in the present study area, SOC and TN concentrations were relatively sufficient according to the classification criteria of the Second National Soil Census in China (Fig. 5; Table 4). However, the soil C and N stocks were not high because of the shallow and discontinuous soils in the karst areas (Jiang *et al.* 2014).

Previous studies have indicated that SOC is closely correlated with TN (Wang *et al.* 2018; Wang R Z *et al.* 2021; Yang *et al.* 2021); therefore, during soil development, SOC and TN co-evolve. Similarly, in the present study, we found that SOC and TN showed similarities in their degrees of variation, spatial autocorrelations, and spatial distribution characteristics (Figs. 2–4). Other soil properties such as Ca^{2+}, pH, and BD were the main drivers of SOC and TN variations (Fig. 6). Furthermore, soil physical and chemical properties were found to regulate soil nutrient cycling, which is similar to the results of most previous studies (Wang *et al.* 2019;

Li *et al.* 2020; Yang *et al.* 2021). Soil BD can reflect soil permeability, aeration, and resistance during root extension (Yang *et al.* 2021), whereas soil pH can directly affect the existing forms, bio-availability, and migration of nutrients (Li *et al.* 2020). In general, BD is strongly correlated with SOC, whereas SOC is significantly correlated with most other soil nutrient indicators, such as TN, also indicated in Table 5 in the present study. Therefore, SOC and TN are usually influenced by similar drivers (Wang R Z *et al.* 2021).

Soil P differs from soil C and N because of the differences in the corresponding nutrient circulations, with P representing a sedimentary mineral element (Zhu *et al.* 2021). Overall, soil TP was moderately deficient (Table 4), similar to the results of Chen *et al.* (2018), who found that both karst and non-karst forests were limited by soil P. K is a major but largely neglected soil nutrient that can limit terrestrial plant productivity, along with N and P (Schlesinger 2021). However, research on K is considerably limited compared with that on N and P. In the present study, soil TK was proven to be deficient because of a high proportion (up to 87.6% of the total) of the area being deficient (Table 4). This could be attributed to the warm and humid climate in this region, which continuously depleted the soil inter-layers and leached K from the soil. Furthermore, higher temperatures and precipitation can enhance plant growth, increase plant K uptake, and consequently reduce K in soil (Chen *et al.* 2020). In summary, compared with soil C and N, plants in the study area were more vulnerable to P and K limitations.

4.3. Soil nutrient variations and major driving factors

Previous studies have quantified soil nutrient variability and its driving factors using geostatistics and spatial analysis (Li *et al.* 2020; Wang *et al.* 2020; Haruna 2021; Wang R Z *et al.* 2021; Zhu *et al.* 2021). In the present study, soil nutrients showed moderate variation, with CVs ranging from 0.60 to 0.72 (Fig. 2). Haruna (2021) evaluated the spatial variability of selected soil macro- and micro-nutrients along a catena based on a semi-variogram analysis and reported that the Gaussian isotropic model was the best fit for all nutrient elements across all slope positions. Wang R Z *et al.* (2021) identified the best-fit semi-variogram models for SOC and TN densities in the desert steppes of China's Hexi Corridor based on geostatistical analysis and also found that Gaussian models were optimal for SOC and TN density in most soil layers. However, in the present study area, the best-fitting semi-variogram models for SOC, TN, TP, and TK were spherical, Gaussian, exponential, and exponential, respectively (Table 3). Furthermore, through spatial autocorrelation and clustering analysis using global and local Moran's indices, Wang *et al.* (2020) indicated that soil and vegetation properties in

Table 5 Correlation analysis among the factors influencing soil nutrients[1)]

Index	Land use	Lithology	Slope position	BD	pH	Clay	SD	Ca^{2+}	MAT	Mg^{2+}	NDVI	y^3	y^2	x^3	Sand	Slope
BD	**		**	1												
pH	**	**		−0.200**	1											
Clay	**	**		0.272**	−0.038	1										
SD	**	**		0.281**	−0.510**	0.138**	1									
Ca^{2+}	**	**		−0.424**	0.680**	−0.053	−0.519**	1								
MAT	**		*	0.128*	0.172**	0.365**	−0.060	0.146**	1							
Mg^{2+}	**	**		−0.252**	0.474**	−0.189**	−0.293**	0.465**	−0.017	1						
NDVI	**		**	−0.092	0.053	−0.101	−0.103	0.005	−0.177**	0.183**	1					
y^3		**	**	−0.112*	−0.276**	−0.459**	0.206**	−0.244**	−0.610**	−0.045	0.079	1				
y^2		**	**	−0.112*	−0.276**	−0.460**	0.206**	−0.244**	−0.611**	−0.043	0.080	1.000**	1			
x^3	*	**	**	−0.101	−0.144**	−0.347**	0.120*	−0.065	−0.070	0.187**	0.007	0.475**	0.478**	1		
Sand	**	**		−0.375**	0.394**	−0.432**	−0.517**	0.382**	−0.055	0.244**	0.082	−0.022	−0.022	−0.023	1	
Slope	**	**		−0.030	0.311**	0.191**	−0.280**	0.226**	0.271**	0.142**	0.064	−0.442**	−0.442**	−0.405**	0.136**	1
SOC	**	**	**	−0.723**	0.451**	−0.444**	−0.504**	0.600**	−0.185**	0.420**	0.189**	0.153**	0.154**	0.071	0.540**	0.091
TN	**	**	**	−0.689**	0.570**	−0.368**	−0.502**	0.684**	−0.121*	0.504**	0.159**	0.073	0.073	0.037	0.495**	0.141**
TP	**	**	**	−0.266**	0.436**	0.063	−0.217**	0.448**	0.060	0.399**	−0.044	−0.212**	−0.211**	−0.112*	0.116*	0.086
TK	**	**		0.028	−0.245**	0.119*	0.387**	−0.172**	−0.215**	−0.208**	0.131*	0.292**	0.290**	−0.137**	−0.293**	−0.104*

[1)] BD, bulk density; SD, soil depth; MAT, mean annual temperature; NDVI, normalized difference vegetation index; y^2, y^3, and x^3, derived variables of longitude x and latitude y; SOC, soil organic carbon; TN, total nitrogen; TP, total phosphorus; TK, total potassium.
The effects of land use, lithology, and slope position on other variables were determined using one-way analysis of variance (ANOVA). The null hypothesis was that land use, lithology, and slope position had no significant effect on the variable. ** represents that the variables are significantly affected by land use, lithology, or slope position at the $P<0.01$ level while * represents $P<0.05$ level.

the Pingshuo opencast coalmine areas in the Loess Plateau of China showed relatively high spatial clustering. Similarly, in the present study, all soil nutrients showed an obvious positive spatial autocorrelation, with GMIs ranging from 0.64 to 0.77 (Fig. 3). The low LMIs indicated large spatial variations in all soil nutrients.

Regarding the quantification of factors influencing soil nutrient variations, Li *et al.* (2020) quantified the effects of climatic factors and soil properties on soil nutrients across the Huang-Huai-Hai River Basin in China and reported that soil pH explained most of the total variation in soil nutrients, whereas climatic factors explained 5.64–28.16% of the variations in soil nutrients, except for available P (0.0%) and TK (68.35%). In the present study, the selected significant (P<0.05) influencing factors explained 58.8% of the total variation in soil nutrients (Fig. 7). In addition, soil properties such as soil mechanical composition and pH, explained soil nutrient variations more effectively than spatial and environmental variables. Soil properties such as soil microbial characteristics (Osburn *et al.* 2021), environmental factors such as air humidity (Li *et al.* 2020), and human activities such as ecological restoration programs (Huang *et al.* 2020) could have been the major influencing factors for the unexplained variations.

The significant influencing factors for soil nutrients included BD, pH, lithology, clay, SD, Ca^{2+}, MAT, Mg^{2+}, NDVI, slope position, y^3, y^2, x^3, sand, and slope (P<0.05). These results are consistent with those of previous studies (Tang *et al*. 2019; Wang *et al.* 2019; Li *et al.* 2020; Yang *et al.* 2021), but notably, geographic location is seldom mentioned in previous studies as an independent variable influencing soil nutrients. Among the aforementioned factors, some directly influenced soil nutrient distributions, whereas others had indirect effects; that is, a correlation existed among the influencing factors, and some variables influenced soil nutrients by affecting some factors directly (Liu *et al.* 2019; Huo *et al.* 2021). For example, Liu *et al.* (2019) studied the changes in soil N stocks following vegetation restoration in a typical karst catchment in Southwest China, and found that BRR affected the changes in soil N by affecting the changes in soil C and directly affecting BD, SD, and Ca^{2+}. In the present study, the spatial variables (y^2, y^3, or x^3) were strongly correlated with lithology, slope position, topography (slope), and climate (MAT) (Table 5). Lithology considerably affects the exchangeable cation (Ca^{2+} and Mg^{2+}) concentration in karst soils (Li *et al.* 2017). Thus, the spatial variables were also significantly correlated with exchangeable cations. In addition, the spatial variables were significantly correlated with SD, BD, pH, and clay content, possibly due to the differences in the parent materials across different regions.

5. Conclusion

This study quantitatively analyzed the spatial distribution characteristics and major driving factors of topsoil nutrients in a typical karst region in Southwest China using descriptive statistics, geostatistics, and spatial analysis. The SOC, TN, TP, and TK concentrations exhibited moderate variations and obvious positive spatial autocorrelations. Low LMI values indicated large spatial variations in soil nutrients. Furthermore, the optimal fitting semi-variogram models for SOC, TN, TP, and TK concentrations were spherical, Gaussian, exponential, and exponential, respectively. According to the classification criteria of the Second National Soil Census in China, SOC and TN were relatively sufficient, TK was deficient, and TP belonged to the medium-deficient level. Therefore, terrestrial ecosystems in the study area were more vulnerable to soil P and K limitations than soil N. Furthermore, ignoring the interactions, compared with spatial and environmental variables, the single effect of other soil properties accounted more for variations in soil nutrients. Thus, these results on the spatial distribution characteristics of soil nutrients and the relative contributions of various factors influencing their variation will aid future research in karst regions and can provide useful guidance for management measures in terrestrial ecosystems.

Acknowledgements

This research was supported by the National Natural Science Foundation of China (U2344201 and 42101316), the Natural Science Foundation of Hunan Province, China (2022JJ40866), and the Outstanding Youth Project of Education Bureau of Hunan Province, China (20B613).

Declaration of competing interest

The authors declare that they have no conflicts of interest.

Declaration of generative AI and AI-assisted technologies in scientific writing

The authors declare that they did not use AI in the preparation and writing of this manuscript.

References

Beven K J, Kirkby M J. 1979. A physically based, variable contributing area model of basin hydrology. *Hydrological Sciences Bulletin*, **24**, 43–69.

Carter M R, Gregorich E G. 2006. *Soil Sampling and Methods of Analysis*. 2nd ed. Chemical Rubber Company Press, Boca Raton, USA.

Chen H, Li D J, Xiao K C, Wang K L. 2018. Soil microbial processes and resource limitation in karst and non-karst forests. *Functional Ecology*, **32**, 1400–1409.

Chen H, Luo P, Wen L, Yang L Q, Wang K L, Li D J. 2017. Determinants of soil extracellular enzyme activity in a karst region, southwest China. *European Journal of Soil Biology*, **80**, 69–76.

Chen X Q, Li T, Lu D J, Cheng L, Zhou J M, Wang H Y. 2020. Estimation of soil available potassium in Chinese agricultural fields using a modified sodium tetraphenyl boron method. *Land Degradation & Development*, **31**, 1737–1748.

Duan L X, Li Z W, Xie H X, Li Z M, Zhang L, Zhou Q. 2020. Large-scale spatial variability of eight soil chemical properties within paddy fields. *Catena*, **188**, 104350.

Filippelli G M. 2008. The global phosphorus cycle: Past, present, and future. *Elements*, **4**, 89–95.

Gallaher R N, Weldon C O, Boswell F C. 1976. A semiautomated procedure for total nitrogen in plant and soil samples. *Soil Science Society of America Journal*, **40**, 887–889.

Haruna S I. 2021. Spatial and fractal characterization of selected soil nutrients along a catena. *Catena*, **204**, 105443.

Heikkinen R K, Luoto M, Virkkala R, Rainio K. 2004. Effects of habitat cover, landscape structure and spatial variables on the abundance of birds in an agricultural-forest mosaic. *Journal of Applied Ecology*, **41**, 824–835.

Hu P L, Zhang W, Chen H S, Xu L, Xiao J, Luo Y Q, Wang K L. 2022. Lithologic control of microbial-derived carbon in forest soils. *Soil Biology and Biochemistry*, **167**, 108600.
Huang C B, Zeng Y X, Wang L C, Wang S Q. 2020. Responses of soil nutrients to vegetation restoration in China. *Regional Environmental Change*, **20**, 82.
Huo J Y, Liu C J, Yu X X, Chen L H, Zheng W G, Yang Y H, Yin C W. 2021. Direct and indirect effects of rainfall and vegetation coverage on runoff, soil loss, and nutrient loss in a semi-humid climate. *Hydrological Processes*, **35**, e13985.
Jiang Q H, Zhou P, Liao C, Liu Y, Liu F. 2020. Spatial pattern of soil erodibility factor (K) as affected by ecological restoration in a typical degraded watershed of Central China. *Science of the Total Environment*, **749**, 141609.
Jiang Z C, Lian Y Q, Qin X Q. 2014. Rocky desertification in Southwest China: Impacts, causes, and restoration. *Earth-Science Reviews*, **132**, 1–12.
Jobbágy E G, Jackson R B. 2000. The vertical distribution of soil organic carbon and its relation to climate and vegetation. *Ecological Applications*, **10**, 423–436.
Li D J, Wen L, Yang L Q, Luo P, Xiao K C, Chen H, Zhang W, He X Y, Chen H S, Wang K L. 2017. Dynamics of soil organic carbon and nitrogen following agricultural abandonment in a karst region. *Journal of Geophysical Research* (Biogeosciences), **122**, 230–242.
Li Y Q, Ma J W, Xiao C, Li Y J. 2020. Effects of climate factors and soil properties on soil nutrients and elemental stoichiometry across the Huang-Huai-Hai River Basin, China. *Journal of Soils and Sediments*, **20**, 1970–1982.
Liu F, Wu H Y, Zhao Y G, Li D C, Yang J L, Song X D, Shi Z, Zhu A X, Zhang G L. 2022. Mapping high resolution National Soil Information Grids of China. *Science Bulletin*, **67**, 328–340.
Liu S J, Zhang W, Wang K L, Pan F J, Yang S, Shu S Y. 2015. Factors controlling accumulation of soil organic carbon along vegetation succession in a typical karst region in Southwest China. *Science of the Total Environment*, **521**, 52–58.
Liu X, Zhang W, Wu M, Ye Y Y, Wang K L, Li D J. 2019. Changes in soil nitrogen stocks following vegetation restoration in a typical karst catchment. *Land Degradation & Development*, **30**, 60–72.
Luo M Y, Wang T W, Li Z Y, Zhang T Y, Yang J W, Li N, Li Z X. 2021. Spatial distribution characteristics of pedodiversity and its major driving factors in China based on analysis units of different sizes. *Catena*, **207**, 105701.
Maila M P, Randima P, Drønen K, Cloete T E. 2006. Soil microbial communities: Influence of geographic location and hydrocarbon pollutants. *Soil Biology and Biochemistry*, **38**, 303–310.
Meng X, Cao J N, Wang X F, Zhang C, Lv J S. 2021. Spatial characteristics of the human factors of soil erosion at the boundary of political divisions: A spatial approach. *Catena*, **201**, 105278.
Osburn E D, Badgley B D, Strahm B D, Aylward F O, Barrett J E. 2021. Emergent properties of microbial communities drive accelerated biogeochemical cycling in disturbed temperate forests. *Ecology*, **102**, e03553.
Schlesinger W H. 2021. Some thoughts on the biogeochemical cycling of potassium in terrestrial ecosystems. *Biogeochemistry*, **154**, 427–432.
Tan Q Q, Chen Y Z, Han W X, Wang G A. 2020. Dynamics of soil metallic nutrients across a 6000-km temperature transect in China. *Science of the Total Environment*, **744**, 140888.
Tang J, Tang X X, Qin Y M, He Q S, Yi Y, Ji Z L. 2019. Karst rocky desertification progress: Soil calcium as a possible driving force. *Science of the Total Environment*, **649**, 1250–1259.
Tang X L, Zhao X, Bai Y F. 2018. Carbon pools in China's terrestrial ecosystems: New estimates based on an intensive field survey. *Proceedings of the National Academy of Sciences of the United States of America*, **115**, 4021–4026.
Wang J M, Ouyang J M, Zhang M. 2020. Spatial distribution characteristics of soil and vegetation in a reclaimed area in an opencast coalmine. *Catena*, **195**, 104773.
Wang L L, Zhang G H, Zhu P Z, Wang Z G. 2023. Correlations of C, N, P contents and their stoichiometry between plant and soil on steep gully slopes. *Ecological Indicators*, **154**, 110545.
Wang M M, Chen H S, Zhang W, Wang K L. 2018. Soil nutrients and stoichiometric ratios as affected by land use and lithology at county scale in a karst area, southwest China. *Science of the Total Environment*, **619**, 1299–1307.
Wang M M, Chen H S, Zhang W, Wang K L. 2019. Influencing factors on soil nutrients at different scales in a karst area. *Catena*, **175**, 411–420.
Wang M R, Liu H J, Lennartz B. 2021. Small-scale spatial variability of hydro-physical properties of natural and degraded peat soils. *Geoderma*, **399**, 115123.
Wang R Z, Yang J J, Liu H Y. 2021. Nitrogen enrichment buffers phosphorus limitation by mobilizing mineral-bound soil phosphorus in grasslands. *Ecology*, **103**, e3616.
Wang X Y, Li Y Q, Duan Y L, Wang L L, Niu Y Y, Li X H, Yan M. 2021. Spatial variability of soil organic carbon and total nitrogen in desert steppes of China's Hexi Corridor. *Frontiers in Environmental Science*, **9**, 761313.
Wen D, He N P. 2016. Forest carbon storage along the north-south transect of eastern China: Spatial patterns, allocation, and influencing factors. *Ecological Indicators*, **61**, 960–967.
WRB (World Reference Base for Soil Resources 2014). 2015. International soil classification system for naming soils and creating legends for soil maps. *World Soil Resources Reports*, **106**, 151–156.
Xie W P, Yang J S, Yao R J, Wang X P. 2021. Spatial and temporal variability of soil salinity in the Yangtze River Estuary using electromagnetic induction. *Remote Sensing*, **13**, 1875.
Yang X, Shao M A, Li T C, Zhang Q Y, Gan M, Chen M Y, Bai X. 2021. Distribution of soil nutrients under typical artificial vegetation in the desert-loess transition zone. *Catena*, **200**, 105165.
Zhang C H, Qi X K, Wang K L, Zhang M Y, Yue Y M. 2017. The application of geospatial techniques in monitoring karst vegetation recovery in southwest China: A review. *Progress in Physical Geography*, **41**, 450–477.
Zhang J, Wang X J, Wang J P. 2014. Impact of land use change on profile distributions of soil organic carbon fractions in the Yanqi Basin. *Catena*, **115**, 79–84.
Zhang M Y, Wang K L, Liu H Y, Zhang C H, Wang J, Yue Y M, Qi X K. 2015. How ecological restoration alters ecosystem services: An analysis of vegetation carbon sequestration in the karst area of Northwest Guangxi, China. *Environmental Earth Sciences*, **74**, 5307–5317.
Zhou Y, Xue J, Chen S C, Zhou Y, Liang Z Z, Wang N, Shi Z. 2020. Fine-resolution mapping of soil total nitrogen across China based on weighted model averaging. *Remote Sensing*, **12**, 85.
Zhu J, Wu A C, Zhou G Y. 2021. Spatial distribution patterns of soil total phosphorus influenced by climatic factors in China's forest ecosystems. *Scientific Reports*, **11**, 5357.

Guest Editor Weiguo Cheng
Managing Editor Lujuan Sun